

Received 26 September 2023, accepted 13 October 2023, date of publication 18 October 2023, date of current version 23 October 2023.

Digital Object Identifier 10.1109/ACCESS.2023.3325485

RESEARCH ARTICLE

Assessing the Causal Effects of Climate Change on Vegetation Dynamics in Northeast China Using Convergence Cross-Mapping

JIAPEI WU^{1,2}, YUKE ZHOU¹, HAN WANG^{1,2}, XIAOYING WANG³, AND JIAOJIAO WANG⁴

¹Key Laboratory of Ecosystem Network Observation and Modeling, Institute of Geographic and Natural Resources Research, Chinese Academy of Sciences, Beijing 100101, China

²University of Chinese Academy of Sciences, Beijing 100049, China

³Institute of Atmospheric Environment, CMA, Shenyang 110166, China

⁴State Key Laboratory of Multimodal Artificial Intelligence Systems, Institute of Automation, Chinese Academy of Sciences, Beijing 100190, China

Corresponding author: Yuke Zhou (zhouyk@igsrr.ac.cn)

This work was supported in part by the National Key Research and Development Program under Grant 2021xjkk0303; in part by the Jointly Open Fund Subsidized by Key Laboratory of Agro-Meteorological Disaster of Liaoning Province and Institute of Atmospheric Environment, China Meteorological Administration, Shenyang, under Grant 2023SYIAEFZD05; and in part by the National Natural Science Foundation of China under Grant 72074209.

ABSTRACT The patterns of interaction between terrestrial vegetation and the atmosphere are complex, and some are poorly understood. Linear or general linear methods have been widely used to explore the dynamics of vegetation and climate changes. However, linear thinking may hinder our understanding of complex nonlinear systems, and it is difficult to extract the underlying causality of linear correlations directly from observational data. In this study, we aimed to quantify the interactions between vegetation and climate, using nonlinear dynamical methods based on state-space reconstruction and datasets from Chinese meteorological stations and remote sensing data during 1982–2015 in Northeast China (NEC). Specifically, we identified the causal links between meteorological factors (temperature and precipitation) and the vegetation index (NDVI) by reconstructing the state space from historical records. During the study period, vegetation exhibited a strong bidirectional causal relationship with both temperature and precipitation across Northeast China. The NDVI can be accurately reconstructed from the state information of meteorological factors (temperature and precipitation). The results of the multivariate EDM scenarios reveal varying sensitivities of different vegetation types to meteorological factors. Overall, slight temperature changes have a stronger impact on vegetation compared to precipitation. Mixed forest and broad-leaved forest demonstrate lower sensitivity to precipitation changes compared to other vegetation types. This study on the causal relationship between vegetation and meteorological factors in Northeast China contributes to a deeper understanding of climate change and vegetation feedback in middle and high latitudes. Our work demonstrates that the EDM-based convergent cross-mapping nonlinear causal analysis method is valuable for comprehending the interactions within complex systems in earth science.

INDEX TERMS Vegetation dynamic, climate change, causal links, convergent cross mapping, empirical dynamic model.

I. INTRODUCTION

Vegetation is an essential component of terrestrial ecosystems, providing important ecological services and impacting

The associate editor coordinating the review of this manuscript and approving it for publication was John Xun Yang¹.

climate feedback [1]. Numerous interconnected biogeochemical processes and land use factors, including biochemical elements that cause regional climate change, are accountable for long-term vegetation alterations, such as temperature, precipitation, and radiation [2]. Vegetation growth responds to alterations in the amount of heat and water that plants receive

as a result of climate change. Conversely, vegetation changes impact climate by modifying the source of surface energy exchanges, increasing friction with near-surface winds, and altering evapotranspiration [3]. Regional vegetation historical records are often considered as evidence of climate change, and the impact of climate change on vegetation can be analyzed from both spatial and temporal perspectives [4]. As rapid global climate change continues, there is increasing interest among researchers in investigating the complex interplay between vegetation and these changes [5], [6], [7], [8]. Nevertheless, the vegetation-atmosphere system is characterized by a range of intricate and dynamic processes, including time-lags between growth and climate [9], interactions between abiotic (environmental) and biotic factors affecting vegetation growth [10], and variations in links between vegetation growth and climate change according to geographical location [11], among others. As such, there remains significant uncertainty when it comes to quantifying cause-effect interactions underlying this complex relationship.

Recent advancements in satellite remote sensing have made it possible to illustrate vegetation dynamics over extensive time periods at regional and global scales [12], [13], [14]. To monitor changes in terrestrial ecosystems, the widely-used Normalized Difference Vegetation Index (NDVI) has been applied as a conventional remote-sensing product [15], [16], [17], [18]. GIMMS NDVI, which has the highest temporal consistency among long-term AVHRR datasets, has been identified as the most practical choice for NDVI trend analysis [19]. It is an effective indicator of vegetation growth status, and is highly correlated with ground biomass at different spatial and temporal scales [20].

Studies on vegetation-atmosphere interactions often depend on either simulation experiments or correlational methods [21]. Simulation experiments require knowledge of the underlying physical equations and can be computationally expensive. Furthermore, they may not completely represent reality, which can limit the conclusions drawn from such studies [22]. Additionally, traditional methods for assessing association focus on prediction and estimation, disregarding the causal mechanisms that can result in ambiguous interpretations and spurious connections between variables. A new field of statistics focused on causal inference offers a suitable mathematical framework for establishing and identifying the connection between causes and effects [23]. Granger causality [24] was initially proposed in economics and has since been broadly applied in studying Earth system science. These applications include measuring the effects of El Niño climate temperature changes on global precipitation [25], analyzing the relationship between North Pacific sea ice and Western Pacific (WP) patterns [26], and assessing how vegetation and snow cover impact surface temperature [27], among others. Nevertheless, the Granger technique can encounter challenges when attempting to apply it to systems with non-stationary or nonlinear processes and deterministic linkages, particularly in dynamic systems with

slight to moderate coupling. This is because the technique requires that the information contained in the causal variable be independently isolated from the larger system [28]. Convergent cross-mapping (CCM) is a nonlinear state space reconstruction-based approach for inferring causality that addresses the limitations of the Granger technique [29]. CCM can manage complex causal relationships among multiple variables in non-linear ecosystems. Because of its high precision in detecting causal correlations between variables and its ability to detect even weak causal relationships in non-linear systems, CCM is extensively used in fields such as ecology, chemistry, medicine, and climate change [30], [31], [32], [33].

The region of Northeast China (NEC), situated in eastern Eurasia, is a representative area for studying terrestrial ecosystems and climate change within the International Geosphere Biosphere Program (IGBP) [34]. It spans a significant east-west bioclimatic gradient, characterized by a predominantly temperate continental climate [35]. Based on pollen records, it can be seen that the vegetation pattern in NEC has undergone multiple changes since the Last Glacial Maximum, owing to global climate change [36]. The distribution and variation of forest net primary productivity in Northeast China are related to different forest types [37], while the growth of *Larix gmelinii* forest is mainly regulated by temperature and precipitation [38]. Consequently, NEC is a crucial region for investigating the effects of climate change on vegetation [39], [40].

This study specifically concentrated on the NEC region, using GIMMS NDVI3g time series data from 1982 to 2015. Our investigation focused on identifying vegetation growth trends and examining dynamic evidence of vegetation-climate coupling feedback. Moreover, we employed a multivariate scenario exploration approach to further examine the sensitivity of vegetation growth to climate change.

II. MATERIALS AND METHODS

A. STUDY AREA

Northeast China (NEC), which includes Heilongjiang, Jilin, Liaoning provinces, and the eastern part of Inner Mongolia, extends from 38°N to 56°N in latitude and 115°E to 135°E in longitude. With a surface area of 1.47 million km², this region exhibits significant natural diversity, including variations in soil composition, vegetation types, climate, and geology. The elevation of the region ranges from 0 to 2667 meters above sea level (Figure 1a). The region's topography consists mainly of plains and mountains, including the Songnen Plain, Liaohe Plain, and Sanjiang Plain in the middle, which are surrounded by the Greater Khingan Mountains, Lesser Khingan Mountains, and Changbai Mountains. The local climate of Northeast China is mainly characterized as a temperate, humid, semi-humid continental monsoon climate, with hot and rainy summers and cold and dry winters [41]. Deciduous broad-leaved forests (25.8%) and grasslands (24.6%) are the dominant vegetation types in Northeast China, while cultivated vegetation (croplands) account for 26.4% (Figure 1b).

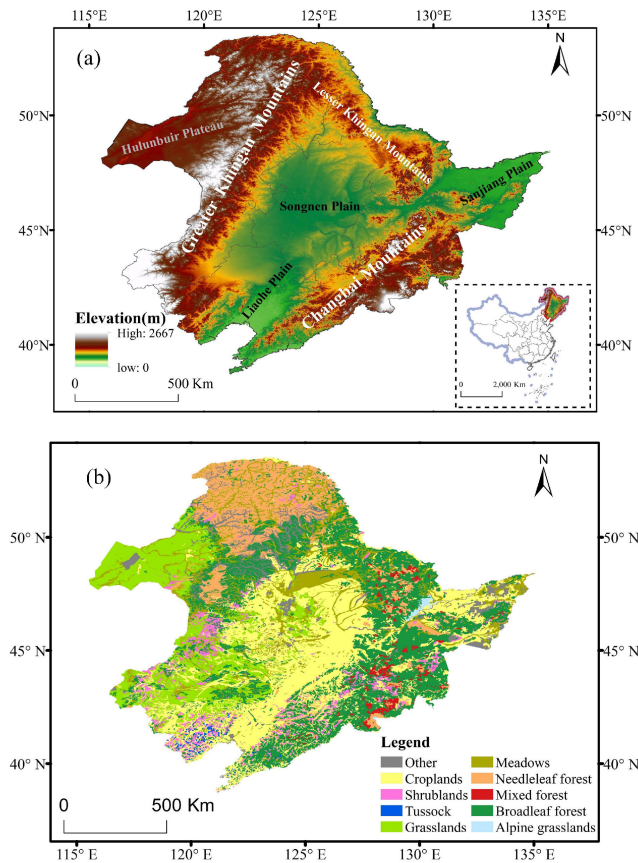


FIGURE 1. (a) Geographic location of study area; (b) vegetation map of the Northeast China.

B. DATA SOURCES

The third generation Global Inventory Monitoring and Modelling System (GIMMS NDVI3g V1.0, <http://ecocast.arc.nasa.gov>) provided the NDVI dataset used in this study. It had a spatial resolution of 1/12° (roughly 8 km) and a 15-day interval for the years 1982 to 2015. GIMMS NDVI 3g data was produced from multiple Advanced Very High-Resolution Radiometer (AVHRR) satellites, which successfully improved accuracy by removing the impacts of atmospheric water vapor, volcanic eruptions, solar altitude angle and sensor sensitivity. GIMMS data set has the best accuracy in temporal changes and is suitable for long-term studies of land surface vegetation changes and coupled climate-vegetation trends [42]. Temperature and precipitation data were acquired from the daily value dataset of Chinese terrestrial climate information provided by the National Meteorological Information Center of the China Meteorological Administration. These climatic data were interpolated and rasterized using ANUSPLINE software with a spatial resolution of 8 km [43]. Monthly average data of NDVI, air temperature, and precipitation were calculated in this study, which have the same spatial and temporal resolution and projection system. The vegetation types in the Northeast China were obtained from the digitized 1:1,000,000 vegetation map of the People’s Republic of China acquired

from the Data Center for Resources and Environmental Sciences, Chinese Academy of Sciences (RESDC) (<http://www.resdc.cn>). In this study, the categories of “wetlands”, “Alpine”, and “no veg” were excluded because they contained too few grids. A total of eight vegetation types remained, including needleleaf forest (NDF), broadleaf forest (BDF), mixed forest (MIX), shrublands (SHL), grasslands (GRS), tussock (TUS), meadows (MEA), and croplands (CRP).

C. TREND ANALYSIS

The Theil-Sen Median method [44], [45] and Mann-Kendall (MK) test [46] were employed to investigate the trends in NDVI and climate in Northeast China. This is a non-parametric test. The requirement of a normal distribution, often employed in trend analysis of long time series data, is not necessary for this method [47], [48], [49]. The formula for calculating the Sen slope for each pixel is described as follows:

$$\text{Slope} = \text{median} \left(\frac{x_j - x_i}{j - i} \right), \quad \forall j > i, \quad (1)$$

where j and i indicates the ordinal number of the month, x_j, x_i are data at different times, Slope is used to describe the change trend of time series data. The positive or negative Slope value indicates whether the NDVI increased or decreased during the study period.

The formula to calculate the Mann-Kend (MK) test statistic S is as follows:

$$S = \sum_{i=1}^{n-1} \sum_{j=i+1}^n \text{sgn}(x_j - x_i), \quad (2)$$

$$\text{sgn}(x_j - x_i) = \begin{cases} +1, & x_j - x_i > 0, \\ 0, & x_j - x_i = 0, \\ -1, & x_j - x_i < 0, \end{cases} \quad (3)$$

where x_j, x_i are the i, j data value of the time series, respectively; n is the number of data samples; sgn is a step function calculated by formula (3). The trend test is performed by the test statistic Z , which is calculated as follows:

$$Z = \begin{cases} \frac{S - 1}{\sqrt{\text{Var}(S)}}, & S > 0, \\ 0, & S = 0, \\ \frac{S + 1}{\sqrt{\text{Var}(S)}}, & S < 0, \end{cases} \quad (4)$$

where, $\text{Var}(S)$ represents the variance of statistic S , which can be calculated as:

$$\text{Var}(S) = (n(n - 1)(2n + 5) - \sum_{i=1}^m t_i(t_i - 1)(2t_i + 5))/18 \quad (5)$$

where n is the number of data in the sequence; m is the number of duplicate data sets in the sequence, and t is the number of duplicate data in the i th duplicate data group. Under the condition of 95% confidence level test, the absolute value of Z takes 1.96 as the threshold, and the combination with Sen slope is shown in Table 1.

TABLE 1. The classification of vegetation change trend.

Slope value	Z value	Trend features
slope > 0.0005	Z > 1.96	Significant increasing
	Z < 1.96	Slight increasing
0.0005 ≥ slope ≥ -0.0005	Z	No change
slope < -0.0005	Z > 1.96	Slight decreasing
	Z < 1.96	Significant decreasing

D. CAUSAL ANALYSIS FOR VEGETATION AND METEOROLOGICAL FACTORS

We employed causal inference techniques based on empirical dynamic models (EDM) to examine the causal relationships between vegetation and meteorological factors.

Our methodology involved the following steps: (1) Non-linearity test using the s-map technique to confirm the nonlinearity of the vegetation-meteorological system; (2) Utilization of the Convergent cross-mapping (CCM) method to establish the causal relationship between vegetation and meteorological factors; (3) The Seasonal Surrogate Test (SST) was performed to assess the presence of a seasonal synchronization effect among variables; (4) Application of Multivariate EDM for enhancing forecasts and exploring scenarios in order to comprehensively examine the impact of meteorological factors on vegetation.

In the subsequent section, we will present a comprehensive description of each step.

1) NONLINEAR TEST

We employed a straightforward non-linear dynamics test called S-maps to confirm that the relationship between vegetation and meteorological factors constitutes a non-linear system rather than a purely stochastic one. S-maps, alternatively referred to as Sequential Locally Weighted Global Linear Maps, characterize the non-linearity of a time series based on the disparity in predictive performance between a non-linear and a linear model [50]. In the S-maps model, the parameter θ represents a non-linear tuning factor, and the model exhibits non-linearity when $\theta > 0$. However, the model reduces to a global linear mapping when $\theta = 0$. Non-linear dynamics are confirmed by quantifying the enhancement in predictive performance ($\Delta\rho$) achieved with various non-linear parameters ($\theta > 0$), as compared to the linear model ($\theta = 0$).

2) CONVERGENT CROSS MAPPING (CCM)

Convergent cross-mapping (CCM) is a novel technique based on the theory of embedding that allows for the detection of nonlinear causality between time series data [29]. CCM is a nearest-neighbor forecasting approach that aims to determine whether the dynamic trajectories two variables exhibit consistent behavior, indicating some level of cross-predictive skill. This consistency is observed when the system revisits similar states or patterns over time, known as dynamic recurrence. In CCM, the system states are typically unknown, but they

can be approximated using trajectory segments found in a trajectory matrix M_Y . This trajectory matrix is constructed based on Takens' embedding theorem [29], which allows for the reconstruction of the underlying dynamics of a system from a single time series.:

$$M_Y = \{Y_t, Y_{t-1}, \dots, Y_{t-(m-1)}\}, \quad (6)$$

where m is the embedding dimension. In this scenario, when there are unit lags between the time series, the value of m corresponds to the length of the segments. It can be optimized by evaluating the self-forecasting performance when predicting points in Y_t based on their nearest neighbors in M_Y . CCM conducts causal analysis and investigates whether X_t is a cause of Y_t by forecasting the points in X_t using other values from X_t . The time indices of these values are determined based on Y_t which serves as a reference for identifying similar states in M_Y . Predictive skills are typically assessed by calculating the average Pearson correlation coefficient (ρ) between time series and their corresponding forecasts.

This study initially employed CCM to analyze the interaction between NDVI and climate factors on a regional scale, aiming to investigate the relationship between vegetation and climate factors in Northeast China as a whole. Subsequently, CCM analysis was performed based on varying vegetation coverage to examine how different types of vegetation respond to climate change. Lastly, for each pixel, CCM skills were computed in various directionalities between NDVI and temperature, NDVI and precipitation, and temperature and precipitation. CCM can detect both bidirectional causality between variables and unidirectional causality, where X affects Y but Y does not affect X . CCM can detect both bidirectional causality between variables and unidirectional causality, where X affects Y but Y does not affect X . Thus, we compared the differences in CCM skill (ρ_{xy} and ρ_{yx}) for different directionalities of each variable pair (X and Y) to examine the variables that have a dominant influence on the interaction. CCM calculations were performed using the "rEDM" package in the R environment (version 1.13.1).

3) SEASONAL SURROGATE TEST (SST)

Even in the absence of an actual causal link [32], a strong correlation in the seasonal cycles of NDVI and meteorological factors can result in high CCM skill values. This phenomenon is referred to as the seasonal synchronization effect [51]. To eliminate any spurious causality resulting from the seasonal synchronization effects, we employed a null test using surrogate time series. The fundamental concept behind the surrogate seasonal test is to generate time series that exhibit the same level of shared seasonality as the meteorological factors. By performing cross mapping between the NDVI time series and these surrogates of meteorological factors, we obtain a null distribution for the CCM skill (ρ). If the CCM skill (ρ) value between NDVI and the actual meteorological factor series is significantly greater than that between NDVI and the surrogate series, it suggests a genuine causal relationship between NDVI and the meteorological

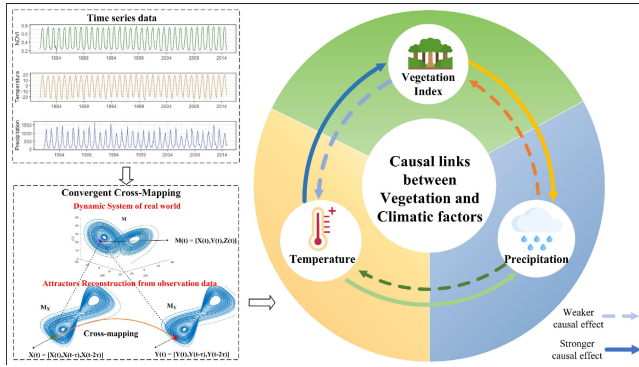


FIGURE 2. Concept diagram of the causal relationship between meteorological and vegetation dynamics (The direction and solidity of the arrows are for illustration only and may not indicate the real relationship).

factor. Finally, a nonparametric one-sample Wilcoxon test was conducted to determine if the relationship between the actual meteorological factor series and NDVI was stronger and statistically significant ($p < 0.05$) compared to the surrogate series.

4) MULTIVIEW EDM

To investigate the causal effect of climate change on vegetation, we employed the multivariate EDM to compare the improvements in multivariate forecasting. This allowed us to assess whether temperature and precipitation had a significant driving effect on NDVI. In essence, Y is considered to have a causal effect on X if incorporating the driving variable Y as a coordinate in the state space results in significantly improved nearest-neighbor predictions for X . In a coupled vegetation-atmosphere system, the variables are not entirely stochastic, implying that some information about the drivers is inherently present in the univariate embedding. Following previous studies [51], we employed a suboptimal embedding dimension E for the multivariate EDM, resulting in a model that does not capture the complete information regarding the system’s state and dynamics. The causal interaction between vegetation and meteorological factors is assessed by calculating the difference in predictions, denoted as

$$\Delta\rho = \rho(\text{with driver}) - \rho(\text{without driver}) \quad (7)$$

Here, ρ represents the Pearson’s correlation between observations and EDM predictions. Besides investigating causality, scenario exploration using multivariate EDM offers an empirical approach to assess the impact of small changes (ΔZ) in meteorological drivers on NDVI. During the scenario exploration step, a multivariate EDM model is constructed to predict NDVI at time t . A meteorological factor with a hypothetical small increase ($+\Delta Z/2$) and decrease ($-\Delta Z/2$) is utilized for this purpose. The difference in predicted NDVI (ΔNDVI), is calculated as:

$$\Delta\text{NDVI} = \text{NDVI}_+(Z(t) + \Delta Z/2) - \text{NDVI}_-(Z(t) - \Delta Z/2) \quad (8)$$

The ratio $\Delta\text{NDVI}/\Delta Z$ quantifies the sensitivity of vegetation to meteorological factors at time t . In this study, we assigned ΔZ values of 0.73°C and 18.94 mm to represent temperature and precipitation, respectively. These values approximately account for 5% of the standard deviation of these variables. During scenario exploration, the embedding dimension E was set to 6.

III. RESULT

A. LONG-TERM CHANGES IN NDVI

Between 1982 and 2015, the vegetation in Northeast China experienced more improvement than degradation at the pixel level (Figure 3a). The Normalized Difference Vegetation Index (NDVI) exhibited an upward trend in 89.6% of the study area, with nearly all pixels (99.6%) showing a significant increase. Only a small number of pixels (3.6%) displayed significant degradation, primarily located sporadically in the northwestern Greater Khingan Mountains, eastern

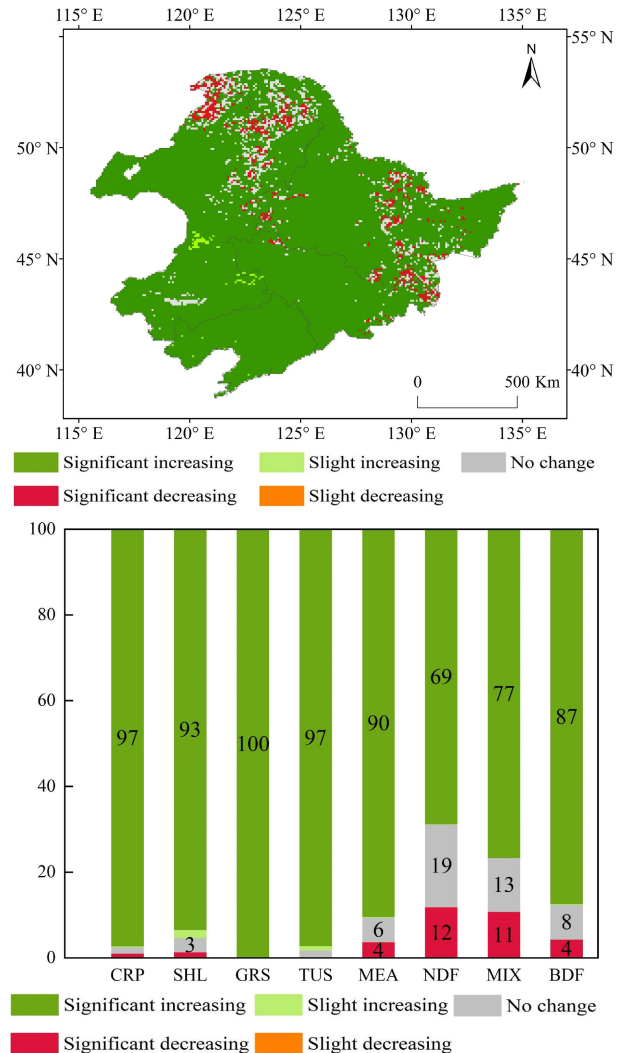


FIGURE 3. (a) Spatial distribution of NDVI changing trend types, (b) the percentage (%) of different types among vegetation types.

Lesser Khingan Mountains, and eastern Changbai Mountains. Forests and meadows were the main vegetation types affected by degradation. At the ecosystem scale (Figure 3b), the majority of forests remained unchanged or degraded in terms of NDVI from 1982 to 2015, with a higher proportion of degraded pixels observed in NDF and MIX (12% and 11%, respectively). Apart from forests, MEA also experienced 4% pixel degradation. The remaining vegetation types exhibited a significant increasing trend.

B. CASUAL LINKS BETWEEN VEGETATION AND METEOROLOGICAL FACTORS

1) NONLINEAR TEST

We examined the non-linearity of vegetation indices and meteorological factors in the Northeast using the S-maps method. The non-linear coordination parameters θ were set to 0.1, 0.3, 0.5, 0.75, and 1.0, while $\Delta\rho$ represented the difference in correlation between the actual and predicted values obtained from the linear and equivalent non-linear models. The results of the non-linearity test (Figure 4) indicate that NDVI, air temperature, and precipitation exhibit non-linear dynamics. In most parts of the northeast, the non-linear model outperformed the linear model ($\Delta\rho > 0$) in terms of predictive performance. Moreover, for both meteorological factors (Tavg and Prec), $\Delta\rho$ increased with higher θ values, suggesting a pronounced non-linearity in these variables. Hence, the coupled system of vegetation and meteorological factors can be regarded as a non-linear dynamical system. Convergent cross-mapping methods can be employed to further investigate evidence of non-linear dynamical causality between them.

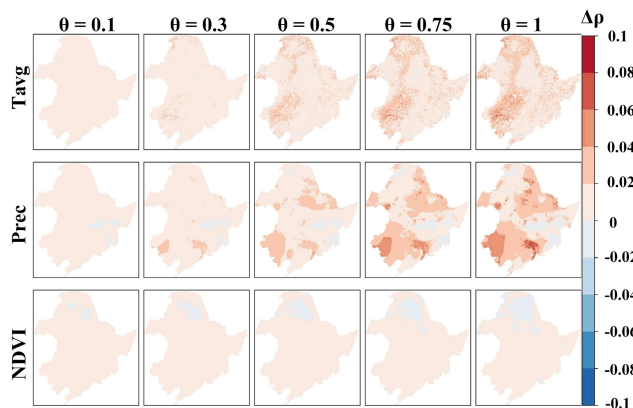


FIGURE 4. Nonlinear test results of NDVI, temperature and precipitation ($\Delta\rho$).

2) REGIONAL CAUSAL RELATIONSHIP BETWEEN VEGETATION AND METEOROLOGICAL FACTORS

We conducted convergent cross-mapping analysis between NDVI and meteorological factors in Northeast China, and compared the results with simple correlation coefficients. The findings provide evidence of convergence between NDVI and temperature as well as precipitation variables. The

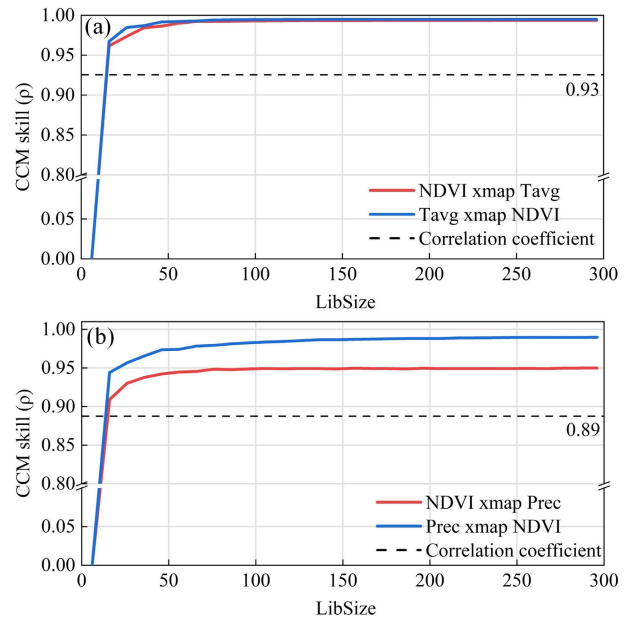


FIGURE 5. The overall cross-map prediction skill between NDVI and meteorological factors. (a)NDVI and Temperature; (b)NDVI and Precipitation.

cross-mapping skills (CCM) exhibited rapid improvement with longer time series lengths, surpassing the performance of correlation coefficients (Figure 5). The cross-mapping skills between NDVI and temperature converge at values of 0.993 and 0.995, respectively. This convergence indicates a strong interaction between NDVI and temperature, as their time series exhibit high similarity. In terms of the cross-mapping skill between NDVI and precipitation, the value of precipitation-mapped NDVI converges to 0.989, which is higher than the value of NDVI-mapped precipitation at 0.951. This suggests that the influence of vegetation on precipitation may be more significant than the driving effect of precipitation on vegetation in Northeast China. Notably, the cross-mapping skills between NDVI and climate factors surpass the correlation coefficients. Consistent with the results of previous studies [52], temperature is the main limiting factor for vegetation growth in Northeast China. This could be attributed to the abundant underlying surface of forests in Northeast China, which exhibits a certain water storage capacity, reducing the impact of forests on precipitation changes. Additionally, the CCM method provides a more comprehensive assessment of causal relationships by estimating the strength of causality in both directions. Thus, it can determine the direction of causal effects.

Seasonal synoptic effects can lead to spurious causality between NDVI and meteorological factors. To address this issue, we generated 1000 seasonal surrogate series for each meteorological factor and performed a significance test between NDVI and the meteorological factors. The test results are shown in Figure 6, where the dashed line represents the CCM skill between NDVI and the actual meteorological factors, and the box plot illustrates the CCM skill

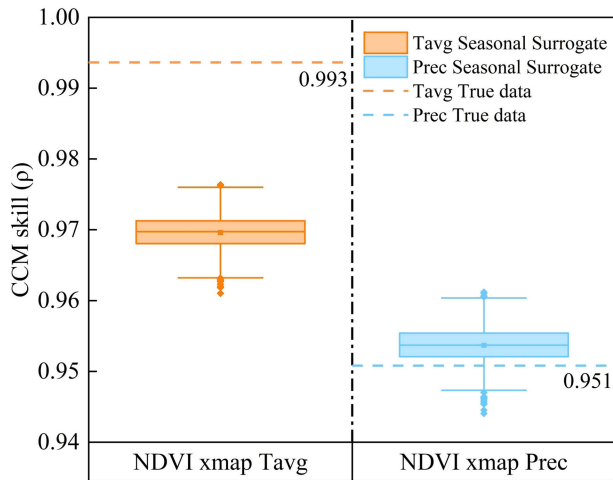


FIGURE 6. Seasonal surrogate test between NDVI and meteorological factors.

between NDVI and the 1000 surrogate series of seasonal meteorological factors. The temperature results demonstrate that the CCM skill of the actual time series is significantly higher than that of the surrogate time series, indicating the absence of a pseudo-causal relationship between NDVI and Tavg. However, it is important to note that the cross-mapping results of NDVI and precipitation may be influenced by shared seasonality, as evidenced by the nonsignificant difference between the CCM skills of the actual time series and the surrogate time series.

3) CAUSAL LINKS BETWEEN VEGETATION AND METEOROLOGICAL FACTORS IN DIFFERENT VEGETATION COVER

Additionally, we investigated the causal relationships between vegetation and meteorological factors in various vegetation cover areas using convergent cross-mapping. The CCM skill value was recorded at convergence for each vegetation type (Figure 7). Similar to the overall CCM results, the CCM skills between different types of vegetation and air temperature were found to be very high. The mapping skills in different directions revealed that NDF, BDF, and SCR types exhibited negative differences, indicating that they are less influenced by temperature compared to their response to temperature. Conversely, MEA, CRL, and STE types showed positive differences, suggesting a stronger response to temperature. Moreover, among all vegetation types, the CCM skill of NDVI cross-mapping with precipitation was smaller than that of precipitation cross-mapping with NDVI. This implies that the impact of vegetation on precipitation is greater than the response of vegetation to precipitation changes. The results of previous studies have confirmed that temperate forests in Northeast China have the ability to regulate the regional water cycle [53]. This is achieved through high evapotranspiration, where forests transfer a significant amount of water to the atmosphere. As a result,

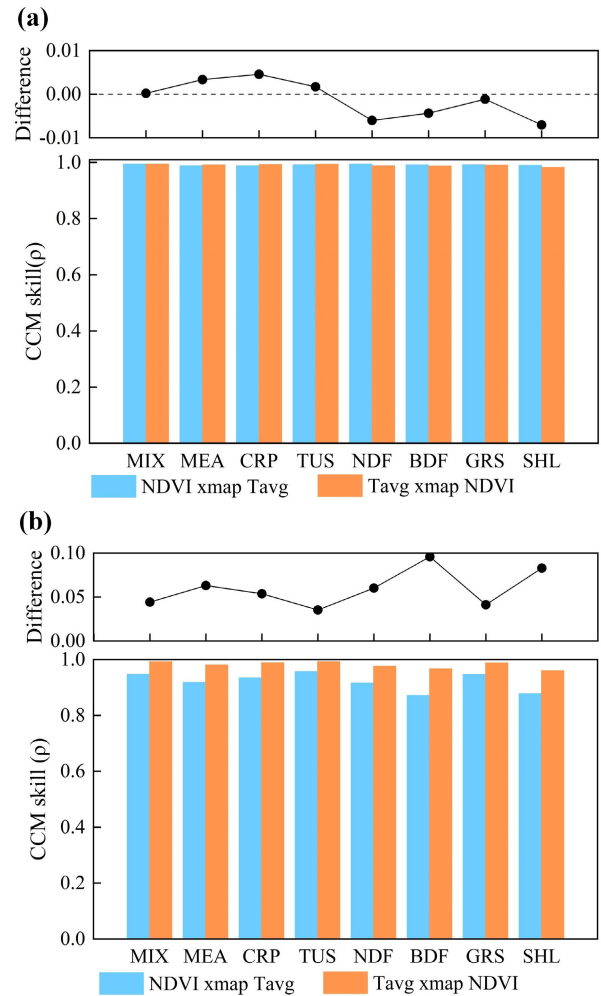


FIGURE 7. Seasonal surrogate test between NDVI and meteorological factors.

this process contributes to an increase in rainfall within the ecosystem.

In addition, Figure 8 shows the time delay corresponding to the maximum cross-mapping skill under different time delays, which partially reflects the time lag effect of the interaction between vegetation and climate factors. Negative time lags were predominant in NDVI cross-mapping with air temperature, indicating a temporal lag in the effect of air temperature on NDVI. In contrast, the best lag values in NDVI to precipitation were both positive and negative, with positive values observed in CRP, BDF, and GRS. However, this does not imply a positive time delay in the causal effect of precipitation on these three vegetation types; instead, it may indicate stronger interactions between precipitation and vegetation leading to this outcome.

4) DISTRIBUTION OF CAUSAL LINKS BETWEEN VEGETATION AND METEOROLOGICAL FACTORS

The cross-mapping skill was utilized as an indicator of causality between NDVI and meteorological factors at the grid scale (Figure 9). A significance test was conducted to determine

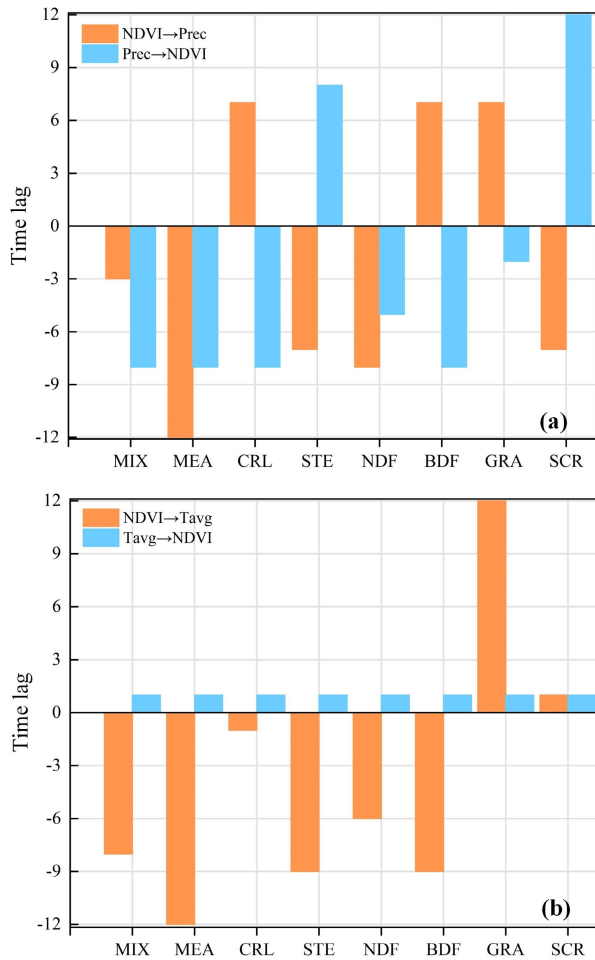


FIGURE 8. The best time lags in different vegetation covers. (a) NDVI and average temperature (Tavg); (b) NDVI and Precipitation (Prec).

the convergence of each grid’s CCM skill, with areas lacking vegetation cover excluded. The results demonstrate that meteorological factors (precipitation and average temperature) had a significant driving influence on vegetation across most of Northeast China. Generally, the strength of the temperature’s driving effect on vegetation gradually increased from north to south, except for the coniferous forest area in the northern section of the Greater Khingan Mountains and the northern section of the Lesser Khingan Mountains, where the effect was comparatively lower. Conversely, the impact of vegetation on temperature was weaker in the southwestern part of the Songnen Plain and the Liaohe Plain, but higher in the rest of the region. Notably, the convergence of NDVI mapping to temperature was statistically significant in 91.1% of the grids, while the convergence of temperature mapping to NDVI passed the significance test in 75.6% of the grids. The discrepancy in NDVI and temperature CCM skills indicates that 81.9% of the regional differences are positive, suggesting that the driving effect of temperature on vegetation surpasses the counter effect of vegetation on temperature in most areas. The cross-mapping skills between NDVI and precipitation exhibited spatial similarity, with low

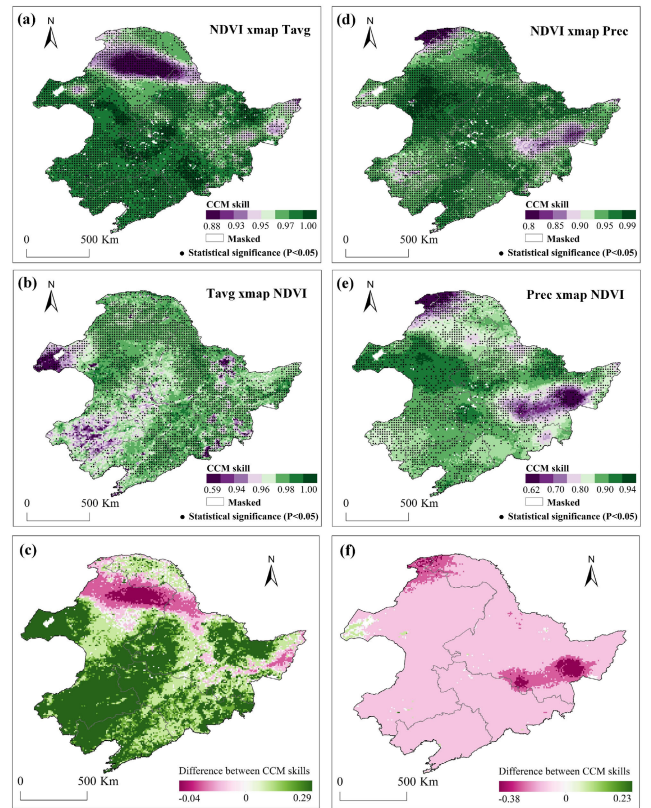


FIGURE 9. Convergence cross-mapping skills of NDVI and meteorological factors on grid scale. (a) NDVI xmap Tavg; (b) Tavg xmap NDVI; (c) difference between CCM skills of NDVI and Tavg cross mapping; (d) NDVI xmap Prec; (e) Prec xmap NDVI; (f) difference between CCM skills of NDVI and Prec cross mapping.

skills observed in the western part of the Sanjiang Plain, the northern part of the Changbai Mountains, and the northernmost part of the Greater Khingan Mountains. For most of these grids, the NDVI xmap Prec and Prec xmap NDVI skills significantly converged (95.9% and 77.2%, respectively). The disparity in mapping skills indicates that nearly all of them are negative (98.5% of total grids), implying that the vegetation’s response to precipitation is smaller than its driving effect.

We utilized improvements in multivariate EDM prediction skills to investigate the causal effects of climate change on vegetation dynamics (Figure 10). The results provide evidence that both monthly average temperature and precipitation act as drivers of NDVI, as the inclusion of either variable enhances forecast skill in most study areas. However, in specific regions such as the Hulunbeier plateau, the western part of the Liaohe Plain, the center of the Songnen Plain, and parts of the Greater Khingan Mountains and Changbai Mountains (approximately 33.27% of the total grids), incorporating precipitation as an embedded coordinate does not lead to a significant improvement in the forecast. The latitudinal distribution reveals the strength of each meteorological factor’s impact on NDVI and its variation with latitude. The influence of temperature on NDVI varies depending on latitude, with a region of lower predicted skill improvement

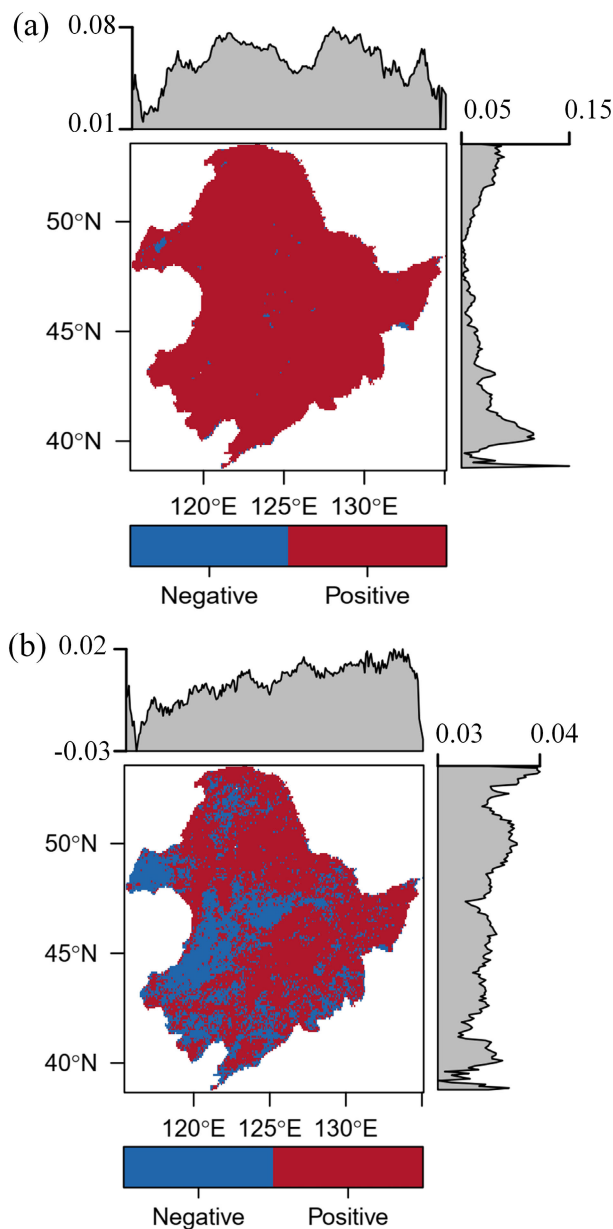


FIGURE 10. Multiview EDM forecast improvement, the two marginal graphics show the column (x) and row (y) averages of the predicted skill improvement, respectively. (a) Temperature leads to improved forecasting skills and (b) precipitation leads to improved forecasting skills.

occurring between 45°N and 50°N, resulting in an overall skill improvement range of 0.05 to 0.15. The effect of precipitation on NDVI is generally weak, with mean values ranging from 0.03 to 0.04.

5) SENSITIVITY OF VEGETATION TO METEOROLOGICAL FACTORS

To investigate the interaction mechanism between vegetation and meteorological factors, we predict the changes in NDVI (ΔNDVI) resulting from slight variations in temperature and precipitation at historical locations. Based on the scenario

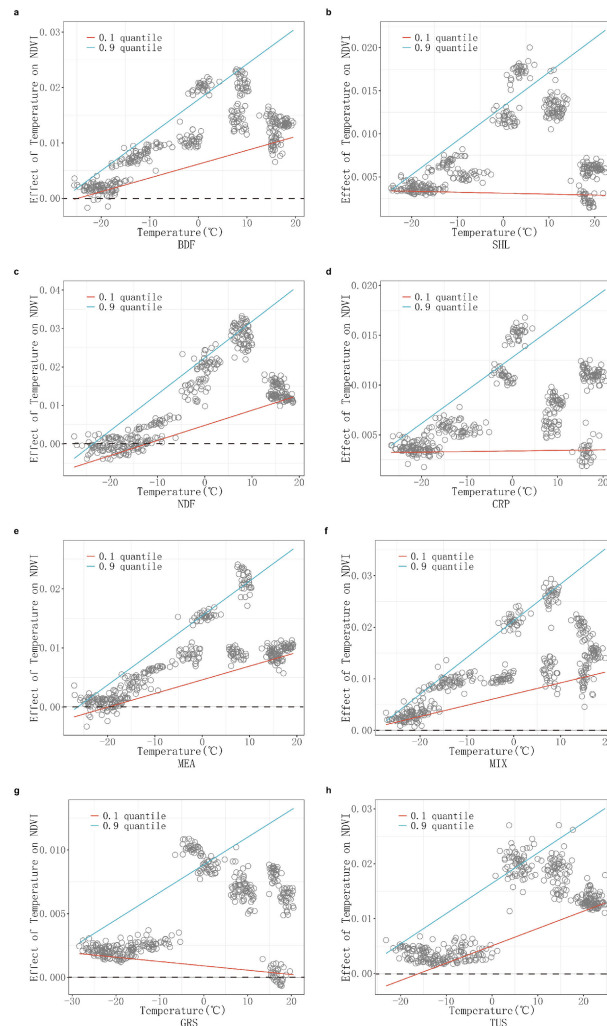


FIGURE 11. Effect of temperature on vegetation ($\Delta\text{NDVI}/\Delta T_{\text{avg}}$) as a function of air temperature. Each point represents the estimated effect of a scenario exploration of a historical point of a vegetation type.

exploration results of various vegetation types influenced by meteorological factors (multivariate EDM), the following findings have been obtained: Firstly, small changes in temperature and precipitation have a positive average influence on vegetation across different vegetation types. The blue and red lines represent the regression results of the 0.9 and 0.1 quantiles, respectively, indicating that temperature and precipitation changes mostly have positive effects on vegetation. Secondly, vegetation exhibited varying responses to temperature and precipitation changes under different hydrothermal conditions. In higher temperature conditions, small temperature changes have a stronger influence on the vegetation dynamics of all vegetation types. In the presence of heavy precipitation, broadleaf forest and mixed forest demonstrated higher sensitivity to precipitation changes, whereas other vegetation types exhibited greater sensitivity to precipitation changes under weak precipitation conditions. Finally, across all vegetation types, vegetation is more strongly

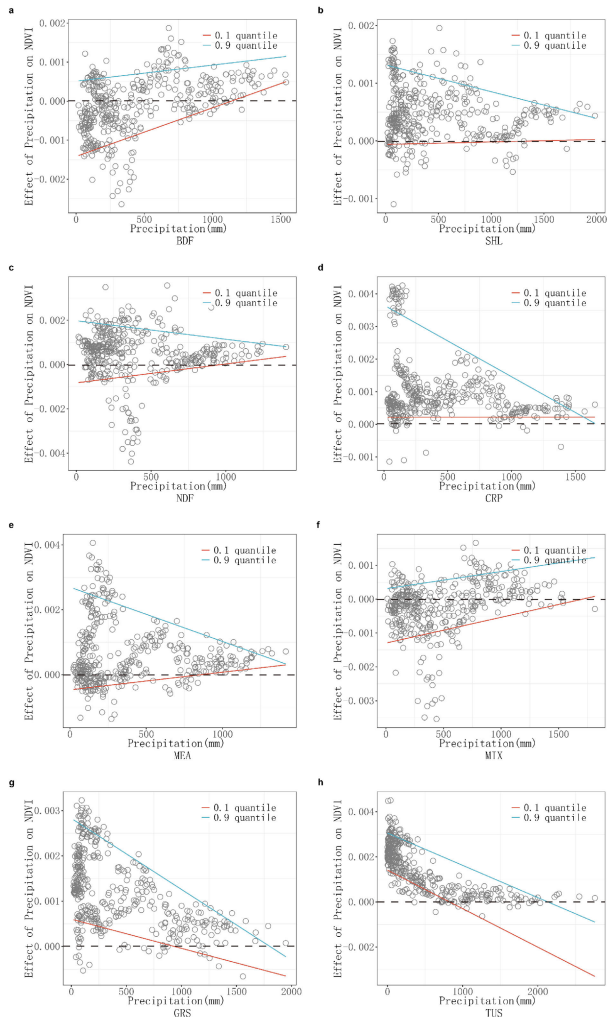


FIGURE 12. Effect of temperature on vegetation ($\Delta\text{NDVI}/\Delta\text{Prec}$) as a function of air temperature. Each point represents the estimated effect of a scenario exploration of a historical point of a vegetation type.

influenced by small changes in temperature than by small changes in precipitation, which aligns with the findings of Convergent Cross Mapping (CCM) discussed in the previous conclusion.

IV. DISCUSSION

A. CASUAL LINKS BETWEEN VEGETATION AND METEOROLOGICAL FACTORS

This study observed a trend of vegetation greening (increasing NDVI over time) in Northeast China from 1982 to 2015, consistent with previous studies [2], [54], [55]. Our results indicate a bidirectional causal relationship between temperature, precipitation, and vegetation growth. One possible explanation is that green vegetation can modify the local climate by influencing variables such as surface energy budget, distribution of sensible heat/latent heat flux, and surface roughness [56]. Increased precipitation can enhance vegetation growth, while vibrant vegetation, in turn, can lead to enhanced evapotranspiration, potentially influencing

the occurrence of precipitation [57]. Vegetation's greenness enhances the evapotranspiration potential, thereby altering temperature through modifications in surface energy. The key factors influencing vegetation growth are "heat and water" conditions, with temperature exerting a more significant impact on vegetation dynamics in NEC than precipitation. The results of CCM and scenario exploration indicate that temperature has a stronger impact on vegetation dynamics than precipitation in NEC. This finding aligns with the results obtained by Mao et al. [58] through site data analysis and may be influenced by the high latitude and climate characteristics of Northeast China. Vegetation growth is limited at high latitudes due to generally cold temperatures. Additionally, elevated temperatures during the growing season stimulate photosynthesis activities and enhance photosynthetic efficiency, thereby promoting vegetation growth [59].

Furthermore, scenario exploration using multivariate EDM reveals varying sensitivities of different vegetation types to temperature and precipitation across diverse hydrothermal conditions. Due to its high latitude and cold climate, temperature serves as the primary limiting factor for vegetation growth in Northeast China. Temperature change predominantly have positive affect on vegetation, with the magnitude of this influence increasing as temperatures transition from negative to positive. However, elevated temperatures can potentially harm plant tissues, decrease photosynthetic rates, and impede plant growth [60]. Plants can undergo physiological adaptations, including alterations in leaf anatomy, stomatal conductance, and photosynthetic rates, in response to high temperatures. Nonetheless, these adjustments may not fully offset the adverse impacts of elevated temperatures [61]. Consequently, under high temperature conditions, the impact of temperature change on vegetation diminishes. The influence of precipitation on vegetation varies across different vegetation types. Broadleaf forests and mixed forests generally exhibit lower sensitivity to precipitation changes compared to other vegetation types. This may be attributed to their deep roots and ample reserves of carbohydrates and nutrients, which reduce their vulnerability to water limitations during severe or prolonged droughts in forest ecosystems [62]. Conversely, due to their shallow root systems, grasslands heavily rely on water resources from the upper soil layers. Improved water availability alleviates water stress and promotes vegetation growth in grassland ecosystems [63].

B. ADVANTAGES OF EDM FOR CAUSAL ANALYSIS IN COMPLEX ECOSYSTEMS

Previous studies investigating the relationship between vegetation dynamics and meteorological factors primarily relied on correlation analysis methods. However, natural systems are often complex and dynamic, exhibiting non-linear behavior that cannot be effectively captured by linear statistical methods. Linear approaches, which are correlation-based, may not be suitable for understanding the intricate dynamics

of systems where causation can exist without correlation and vice versa. To address this limitation, this study employed empirical dynamic modeling (EDM) to explore the causal relationship between vegetation and meteorological factors. The results of the CCM analysis demonstrate that temperature and precipitation have a significant influence on vegetation changes, which is consistent with previous studies [65], [66]. Likewise, vegetation dynamics also affect meteorological factors such as precipitation and temperature, suggesting a bidirectional causal relationship between vegetation and meteorological factors. This result is consistent with previous studies on the sensitivity of vegetation greening observed in China [67], providing further evidence for the effectiveness of EDM in exploring causal relationships within atmospheric ecological systems.

C. LIMITATION

The extended duration of this study (1982-2015), during which human activities have influenced vegetation changes, may pose a potential confounding factor when inferring causality. Nevertheless, in the majority of areas, the existence of nature reserves and native forests eliminated these confounding factors, thereby reflecting the natural vegetation processes that have occurred during the past 34 years. Concurrently, approaches based on the empirical dynamic model (EDM) investigate causal relationships within systems using time series data. However, when applied to raster scales, the interactions among target variables in different domains introduce uncertainty in causal inference. Future studies may consider examining interactions between adjacent domains to enhance the accuracy of causal inference and further investigate the causal effects of human activities on vegetation dynamics.

V. CONCLUSION

Using the Sen-slope and Mann-Kendall methods, we analyzed the trends in NDVI in Northeast China. Throughout the study period, there was a significant increase in NDVI across most areas of Northeast China, except for minor degradation observed in coniferous, broadleaf, and mixed forest cover. Subsequently, we employed a convergent cross-mapping method to infer causal relationships between NDVI and monthly meteorological data from 1982 to 2015. Generally, vegetation dynamics exhibit bidirectional causality with temperature and precipitation; however, the causality between precipitation and vegetation is influenced by the same seasonal cycle to a lesser extent. Our findings indicate that the strength of the causal relationships between vegetation growth and meteorological factors varies among different vegetation covers. Coniferous forest, broadleaf forest, and shrubland exhibited negative differences in cross-mapping with temperature, suggesting that their response to temperature changes was weaker than the driving effect. Additionally, the causal effect of temperature on vegetation typically exhibits time lags. Moreover, we examined the spatial distribution of the causal effects between vegetation and

meteorological variables. The results indicate a bidirectional causal relationship between meteorological factors (temperature and precipitation) and vegetation in the majority of Northeast China. Furthermore, the causal effect of temperature on NDVI showed a stronger impact than precipitation. Findings from scenario exploration unveiled an intricate interaction among meteorological factors (temperature and precipitation) and vegetation. The impact of an individual meteorological factor on vegetation was affected by another factor. This innovative and effective method of nonlinear dynamics offers a novel perspective on the intricate causality that exists between ecological and climatic systems. The approach based on the dynamic empirical model (EDM) can accurately identify and distinguish the causal relationships between vegetation and meteorological factors.

REFERENCES

- [1] S. Piao, J. Wang, X. Li, H. Xu, and Y. Zhang, "Spatio-temporal changes in the speed of canopy development and senescence in temperate China," *Global Change Biol.*, vol. 28, no. 24, pp. 7366–7375, Dec. 2022, doi: [10.1111/gcb.16408](https://doi.org/10.1111/gcb.16408).
- [2] Z. Zhu et al., "Greening of the Earth and its drivers," *Nature Climate Change*, vol. 6, no. 8, pp. 791–795, Aug. 2016, doi: [10.1038/nclimate3004](https://doi.org/10.1038/nclimate3004).
- [3] R. A. McPherson, "A review of vegetation-atmosphere interactions and their influences on mesoscale phenomena," *Prog. Phys. Geography, Earth Environ.*, vol. 31, no. 3, pp. 261–285, 2007, doi: [10.1177/0309133307079055](https://doi.org/10.1177/0309133307079055).
- [4] G. Bao, Y. Bao, A. Sanjjava, Z. Qin, Y. Zhou, and G. Xu, "NDVI-indicated long-term vegetation dynamics in Mongolia and their response to climate change at biome scale," *Int. J. Climatol.*, vol. 35, no. 14, pp. 4293–4306, Nov. 2015, doi: [10.1002/joc.4286](https://doi.org/10.1002/joc.4286).
- [5] Y. H. Fu, H. Zhao, S. Piao, M. Peaucelle, S. Peng, G. Zhou, P. Ciais, M. Huang, A. Menzel, J. Peñuelas, Y. Song, Y. Vitasse, Z. Zeng, and I. A. Janssens, "Declining global warming effects on the phenology of spring leaf unfolding," *Nature*, vol. 526, no. 7571, pp. 104–107, Oct. 2015, doi: [10.1038/nature15402](https://doi.org/10.1038/nature15402).
- [6] W. Cramer, A. Bondeau, F. I. Woodward, I. C. Prentice, R. A. Betts, V. Brovkin, P. M. Cox, V. Fisher, J. A. Foley, A. D. Friend, C. Kucharik, M. R. Lomas, N. Ramankutty, S. Sitch, B. Smith, A. White, and C. Young-Molling, "Global response of terrestrial ecosystem structure and function to CO₂ and climate change: Results from six dynamic global vegetation models," *Global Change Biol.*, vol. 7, no. 4, pp. 357–373, Apr. 2001, doi: [10.1046/j.1365-2486.2001.00383.x](https://doi.org/10.1046/j.1365-2486.2001.00383.x).
- [7] C. Chen, B. He, L. Guo, Y. Zhang, X. Xie, and Z. Chen, "Identifying critical climate periods for vegetation growth in the Northern Hemisphere," *J. Geophys. Res., Biogeosci.*, vol. 123, no. 8, pp. 2541–2552, Aug. 2018, doi: [10.1029/2018JG004443](https://doi.org/10.1029/2018JG004443).
- [8] Y. H. Fu, S. Piao, N. Delapierre, F. Hao, H. Hänninen, Y. Liu, W. Sun, I. A. Janssens, and M. Campioli, "Larger temperature response of autumn leaf senescence than spring leaf-out phenology," *Global Change Biol.*, vol. 24, no. 5, pp. 2159–2168, May 2018, doi: [10.1111/gcb.14021](https://doi.org/10.1111/gcb.14021).
- [9] J. Zhao, S. Huang, Q. Huang, H. Wang, G. Leng, and W. Fang, "Time-lagged response of vegetation dynamics to climatic and teleconnection factors," *Catena*, vol. 189, Jun. 2020, Art. no. 104474, doi: [10.1016/j.catena.2020.104474](https://doi.org/10.1016/j.catena.2020.104474).
- [10] Q.-P. Zhang, J. Wang, and Q. Wang, "Effects of abiotic factors on plant diversity and species distribution of alpine meadow plants," *Ecol. Informat.*, vol. 61, Mar. 2021, Art. no. 101210, doi: [10.1016/j.ecoinf.2021.101210](https://doi.org/10.1016/j.ecoinf.2021.101210).
- [11] J. K. Green, A. G. Konings, S. H. Alemohammad, J. Berry, D. Entekhabi, J. Kolassa, J.-E. Lee, and P. Gentine, "Regionally strong feedbacks between the atmosphere and terrestrial biosphere," *Nature Geosci.*, vol. 10, no. 6, pp. 410–414, Jun. 2017, doi: [10.1038/ngeo2957](https://doi.org/10.1038/ngeo2957).
- [12] S. L. Piao and J. Y. Fang, "Dynamic vegetation cover change over the last 18 years in China," *Quaternary Sci.*, vol. 21, no. 4, pp. 294–302, 2001.

- [13] N. Linscheid, L. M. Estupinan-Suarez, A. Brenning, N. Carvalhais, F. Cremer, F. Gans, A. Rammig, M. Reichstein, C. A. Sierra, and M. D. Mahecha, "Towards a global understanding of vegetation–climate dynamics at multiple timescales," *Biogeosciences*, vol. 17, no. 4, pp. 945–962, Feb. 2020, doi: [10.5194/bg-17-945-2020](https://doi.org/10.5194/bg-17-945-2020).
- [14] D. Fan, L. Ni, X. Jiang, S. Fang, H. Wu, and X. Zhang, "Spatiotemporal analysis of vegetation changes along the belt and road initiative region from 1982 to 2015," *IEEE Access*, vol. 8, pp. 122579–122588, 2020, doi: [10.1109/ACCESS.2020.3007073](https://doi.org/10.1109/ACCESS.2020.3007073).
- [15] Y. Zeng, D. Hao, A. Huete, B. Dechant, J. Berry, J. M. Chen, J. Joiner, C. Frankenberg, B. Bond-Lamberty, Y. Ryu, J. Xiao, G. R. Asrar, and M. Chen, "Optical vegetation indices for monitoring terrestrial ecosystems globally," *Nature Rev. Earth Environ.*, vol. 3, no. 7, pp. 477–493, May 2022, doi: [10.1038/s43017-022-00298-5](https://doi.org/10.1038/s43017-022-00298-5).
- [16] R. Fensholt and S. R. Proud, "Evaluation of Earth observation based global long term vegetation trends—Comparing GIMMS and MODIS global NDVI time series," *Remote Sens. Environ.*, vol. 119, pp. 131–147, Apr. 2012, doi: <https://doi.org/10.1016/j.rse.2011.12.015>.
- [17] J. Verbesselt, R. Hyndman, G. Newnham, and D. Culvenor, "Detecting trend and seasonal changes in satellite image time series," *Remote Sens. Environ.*, vol. 114, no. 1, pp. 106–115, Jan. 2010, doi: [10.1016/j.rse.2009.08.014](https://doi.org/10.1016/j.rse.2009.08.014).
- [18] I. Garonna, R. de Jong, and M. E. Schaepman, "Variability and evolution of global land surface phenology over the past three decades (1982–2012)," *Global Change Biol.*, vol. 22, no. 4, pp. 1456–1468, Apr. 2016, doi: [10.1111/gcb.13168](https://doi.org/10.1111/gcb.13168).
- [19] F. Tian, R. Fensholt, J. Verbesselt, K. Grogan, S. Horion, and Y. Wang, "Evaluating temporal consistency of long-term global NDVI datasets for trend analysis," *Remote Sens. Environ.*, vol. 163, pp. 326–340, Jun. 2015, doi: [10.1016/j.rse.2015.03.031](https://doi.org/10.1016/j.rse.2015.03.031).
- [20] E. Guo, Y. Wang, C. Wang, Z. Sun, Y. Bao, N. Mandula, B. Jirigala, Y. Bao, and H. Li, "NDVI indicates long-term dynamics of vegetation and its driving forces from climatic and anthropogenic factors in Mongolian Plateau," *Remote Sens.*, vol. 13, no. 4, p. 688, Feb. 2021, doi: [10.3390/rs13040688](https://doi.org/10.3390/rs13040688).
- [21] J. Runge et al., "Inferring causation from time series in Earth system sciences," *Nature Commun.*, vol. 10, no. 1, p. 2553, Jun. 2019, doi: [10.1038/s41467-019-10105-3](https://doi.org/10.1038/s41467-019-10105-3).
- [22] J. Runge, V. Petoukhov, J. F. Donges, J. Hlinka, N. Jaycay, M. Vejmelka, D. Hartman, N. Marwan, M. Paluš, and J. Kurths, "Identifying causal gateways and mediators in complex spatio-temporal systems," *Nature Commun.*, vol. 6, no. 1, p. 8502, Oct. 2015, doi: [10.1038/ncomms9502](https://doi.org/10.1038/ncomms9502).
- [23] A. Pérez-Suay and G. Camps-Valls, "Causal inference in geoscience and remote sensing from observational data," *IEEE Trans. Geosci. Remote Sens.*, vol. 57, no. 3, pp. 1502–1513, Mar. 2019, doi: [10.1109/TGRS.2018.2867002](https://doi.org/10.1109/TGRS.2018.2867002).
- [24] C. W. J. Granger, "Investigating causal relations by econometric models and cross-spectral methods," *Econometrica*, vol. 37, no. 3, pp. 424–438, Aug. 1969, doi: [10.2307/1912791](https://doi.org/10.2307/1912791).
- [25] F. N. Silva, D. A. Vega-Oliveros, X. Yan, A. Flammini, F. Menczer, F. Radicchi, B. Kravitz, and S. Fortunato, "Detecting climate teleconnections with Granger causality," *Geophys. Res. Lett.*, vol. 48, no. 18, Sep. 2021, Art. no. e2021GL094707, doi: [10.1029/2021GL094707](https://doi.org/10.1029/2021GL094707).
- [26] N. J. Matthewman and G. Magnusdottir, "Observed interaction between Pacific sea ice and the Western Pacific pattern on intraseasonal time scales," *J. Climate*, vol. 24, no. 19, pp. 5031–5042, Oct. 2011, doi: [10.1175/2011JCLI4216.1](https://doi.org/10.1175/2011JCLI4216.1).
- [27] R. K. Kaufmann, L. Zhou, R. B. Myneni, C. J. Tucker, D. Slayback, N. V. Shabanov, and J. Pinzon, "The effect of vegetation on surface temperature: A statistical analysis of NDVI and climate data," *Geophys. Res. Lett.*, vol. 30, no. 22, p. 2147, Nov. 2003, doi: [10.1029/2003GL018251](https://doi.org/10.1029/2003GL018251).
- [28] H. Ma, S. Leng, C. Tao, X. Ying, J. Kurths, Y.-C. Lai, and W. Lin, "Detection of time delays and directional interactions based on time series from complex dynamical systems," *Phys. Rev. E, Stat. Phys. Plasmas Fluids Relat. Interdiscip. Top.*, vol. 96, no. 1, Jul. 2017, Art. no. 012221, doi: [10.1103/PhysRevE.96.012221](https://doi.org/10.1103/PhysRevE.96.012221).
- [29] G. Sugihara, R. May, H. Ye, C.-H. Hsieh, E. Deyle, M. Fogarty, and S. Munch, "Detecting causality in complex ecosystems," *Science*, vol. 338, no. 6106, pp. 496–500, Oct. 2012, doi: [10.1126/science.1227079](https://doi.org/10.1126/science.1227079).
- [30] Z. Cao, S. Mu, L. Xu, M. Shao, and H. Qu, "Causal research on soil temperature and moisture content at different depths," *IEEE Access*, vol. 9, pp. 39077–39088, 2021, doi: [10.1109/ACCESS.2021.3064264](https://doi.org/10.1109/ACCESS.2021.3064264).
- [31] A. A. Tsonis, E. R. Deyle, R. M. May, G. Sugihara, K. Swanson, J. D. Verbeten, and G. Wang, "Dynamical evidence for causality between galactic cosmic rays and interannual variation in global temperature," *Proc. Nat. Acad. Sci. USA*, vol. 112, no. 11, pp. 3253–3256, Mar. 2015, doi: [10.1073/pnas.1420291112](https://doi.org/10.1073/pnas.1420291112).
- [32] Y. Yu, G. Shang, S. Duan, W. Yu, J. Labeled, and Z. Li, "Quantifying the influences of driving factors on land surface temperature during 2003–2018 in China using convergent cross mapping method," *Remote Sens.*, vol. 14, no. 14, p. 3280, Jul. 2022.
- [33] L. Luo, F. Cheng, T. Qiu, and J. Zhao, "Refined convergent cross-mapping for disturbance propagation analysis of chemical processes," *Comput. Chem. Eng.*, vol. 106, pp. 1–16, Nov. 2017, doi: [10.1016/j.compchemeng.2017.03.026](https://doi.org/10.1016/j.compchemeng.2017.03.026).
- [34] G. Krimmer, N. Viovy, N. de Noblet-Ducoudré, J. Ogée, J. Polcher, P. Friedlingstein, P. Ciais, S. Sitch, and I. C. Prentice, "A dynamic global vegetation model for studies of the coupled atmosphere-biosphere system," *Global Biogeochem. Cycles*, vol. 19, no. 1, Mar. 2005, Art. no. GB1015, doi: [10.1029/2003GB002199](https://doi.org/10.1029/2003GB002199).
- [35] J. Ni and X.-S. Zhang, "Climate variability, ecological gradient and the Northeast China Transect (NECT)," *J. Arid Environ.*, vol. 46, no. 3, pp. 313–325, Nov. 2000, doi: [10.1006/jare.2000.0667](https://doi.org/10.1006/jare.2000.0667).
- [36] X. Li, C. Zhao, and X. Zhou, "Vegetation pattern of northeast China during the special periods since the last glacial maximum," *Sci. China Earth Sci.*, vol. 62, no. 8, pp. 1224–1240, Aug. 2019, doi: [10.1007/s11430-018-9347-3](https://doi.org/10.1007/s11430-018-9347-3).
- [37] J. Zhao, X. Yan, J. Guo, and G. Jia, "Evaluating spatial–temporal dynamics of net primary productivity of different forest types in northeastern China based on improved FORCCHN," *PLoS ONE*, vol. 7, no. 11, Nov. 2012, Art. no. e48131.
- [38] B. Jia, H. Sun, H. H. Shugart, Z. Xu, P. Zhang, and G. Zhou, "Growth variations of Dahurian larch plantations across northeast China: Understanding the effects of temperature and precipitation," *J. Environ. Manage.*, vol. 292, Aug. 2021, Art. no. 112739, doi: [10.1016/j.jenvman.2021.112739](https://doi.org/10.1016/j.jenvman.2021.112739).
- [39] J. Zhao, Y. Wang, Z. Zhang, H. Zhang, X. Guo, S. Yu, W. Du, and F. Huang, "The variations of land surface phenology in northeast China and its responses to climate change from 1982 to 2013," *Remote Sens.*, vol. 8, no. 5, p. 400, May 2016, doi: [10.3390/rs8050400](https://doi.org/10.3390/rs8050400).
- [40] M. Yuan, L. Zhao, A. Lin, L. Wang, Q. Li, D. She, and S. Qu, "Impacts of preseason drought on vegetation spring phenology across the Northeast China Transect," *Sci. Total Environ.*, vol. 738, Oct. 2020, Art. no. 140297, doi: [10.1016/j.scitotenv.2020.140297](https://doi.org/10.1016/j.scitotenv.2020.140297).
- [41] X. Shen, Z. Xue, M. Jiang, and X. Lu, "Spatiotemporal change of vegetation coverage and its relationship with climate change in freshwater marshes of Northeast China," *Wetlands*, vol. 39, no. 3, pp. 429–439, Jun. 2019, doi: [10.1007/s13157-018-1072-z](https://doi.org/10.1007/s13157-018-1072-z).
- [42] H. E. Beck, T. R. McVicar, A. I. J. M. van Dijk, J. Schellekens, R. A. M. de Jeu, and L. A. Bruijnzeel, "Global evaluation of four AVHRR-NDVI data sets: Intercomparison and assessment against Landsat imagery," *Remote Sens. Environ.*, vol. 115, no. 10, pp. 2547–2563, Oct. 2011, doi: [10.1016/j.rse.2011.05.012](https://doi.org/10.1016/j.rse.2011.05.012).
- [43] J. Wang, J. Dong, Y. Yi, G. Lu, J. Oyler, W. K. Smith, M. Zhao, J. Liu, and S. Running, "Decreasing net primary production due to drought and slight decreases in solar radiation in China from 2000 to 2012," *J. Geophys. Res., Biogeosci.*, vol. 122, no. 1, pp. 261–278, Jan. 2017, doi: [10.1002/2016JG003417](https://doi.org/10.1002/2016JG003417).
- [44] H. Theil, "A rank-invariant method of linear and polynomial regression analysis," in *Henri Theil's Contributions to Economics and Econometrics: Econometric Theory and Methodology*, B. Raj and J. Koerts, Eds. Dordrecht, The Netherlands: Springer, 1992, pp. 345–381.
- [45] P. K. Sen, "Estimates of the regression coefficient based on Kendall's tau," *J. Amer. Stat. Assoc.*, vol. 63, no. 324, pp. 1379–1389, Dec. 1968, doi: [10.1080/01621459.1968.10480934](https://doi.org/10.1080/01621459.1968.10480934).
- [46] M. G. Kendall, "Rank correlation methods," in *Public Program Analysis*. Boston, MA, USA: Springer, 1948.
- [47] I. H. Myers-Smith et al., "Complexity revealed in the greening of the Arctic," *Nature Climate Change*, vol. 10, no. 2, pp. 106–117, Feb. 2020, doi: [10.1038/s41558-019-0688-1](https://doi.org/10.1038/s41558-019-0688-1).
- [48] M. Masiol, S. Squizzato, D. C. Chalupa, M. J. Utell, D. Q. Rich, and P. K. Hopke, "Long-term trends in submicron particle concentrations in a metropolitan area of the Northeastern United States," *Sci. Total Environ.*, vol. 633, pp. 59–70, Aug. 2018, doi: [10.1016/j.scitotenv.2018.03.151](https://doi.org/10.1016/j.scitotenv.2018.03.151).

- [49] Q. Liu, X. Wang, Y. Zhang, H. Zhang, and L. Li, "Vegetation degradation and its driving factors in the farming–pastoral ecotone over the countries along belt and road initiative," *Sustainability*, vol. 11, no. 6, p. 1590, Mar. 2019, doi: [10.3390/su11061590](https://doi.org/10.3390/su11061590).
- [50] G. Sugihara, B. T. Grenfell, R. M. May, and H. Tong, "Nonlinear forecasting for the classification of natural time series," *Phil. Trans. Roy. Soc. London. A, Phys. Eng. Sci.*, vol. 348, no. 1688, pp. 477–495, 1994, doi: [10.1098/rsta.1994.0106](https://doi.org/10.1098/rsta.1994.0106).
- [51] E. R. Deyle, M. C. Maher, R. D. Hernandez, S. Basu, and G. Sugihara, "Global environmental drivers of influenza," *Proc. Nat. Acad. Sci. USA*, vol. 113, no. 46, pp. 13081–13086, Nov. 2016, doi: [10.1073/pnas.1607747113](https://doi.org/10.1073/pnas.1607747113).
- [52] H. Li, H. Zhang, Q. Li, J. Zhao, X. Guo, H. Ying, G. Deng, W. Rihan, and S. Wang, "Vegetation productivity dynamics in response to climate change and human activities under different topography and land cover in Northeast China," *Remote Sens.*, vol. 13, no. 5, p. 975, Mar. 2021.
- [53] Y. Jiao, K. Bu, J. Yang, G. Li, L. Shen, T. Liu, L. Yu, S. Zhang, and H. Zhang, "Biophysical effects of temperate forests in regulating regional temperature and precipitation pattern across Northeast China," *Remote Sens.*, vol. 13, no. 23, p. 4767, Nov. 2021.
- [54] S. Piao, G. Yin, J. Tan, L. Cheng, M. Huang, Y. Li, R. Liu, J. Mao, R. B. Myneni, S. Peng, B. Poulter, X. Shi, Z. Xiao, N. Zeng, Z. Zeng, and Y. Wang, "Detection and attribution of vegetation greening trend in China over the last 30 years," *Global Change Biol.*, vol. 21, no. 4, pp. 1601–1609, Apr. 2015, doi: [10.1111/gcb.12795](https://doi.org/10.1111/gcb.12795).
- [55] K. Zheng, L. Tan, Y. Sun, Y. Wu, Z. Duan, Y. Xu, and C. Gao, "Impacts of climate change and anthropogenic activities on vegetation change: Evidence from typical areas in China," *Ecol. Indicators*, vol. 126, Jul. 2021, Art. no. 107648, doi: [10.1016/j.ecolind.2021.107648](https://doi.org/10.1016/j.ecolind.2021.107648).
- [56] G. Forzieri et al., "Increased control of vegetation on global terrestrial energy fluxes," *Nature Climate Change*, vol. 10, no. 4, pp. 356–362, Apr. 2020, doi: [10.1038/s41558-020-0717-0](https://doi.org/10.1038/s41558-020-0717-0).
- [57] X. Zhang, X. Liu, J. Chen, Q. Tang, and Y. Wang, "Responses and feedbacks of vegetation dynamics to precipitation anomaly over the semi-arid area of North China: Evidences from simulations of the WRF-Noah model," *Int. J. Climatol.*, vol. 43, no. 2, pp. 804–817, Feb. 2023, doi: [10.1002/joc.7830](https://doi.org/10.1002/joc.7830).
- [58] D. Mao, Z. Wang, L. Luo, and C. Ren, "Integrating AVHRR and MODIS data to monitor NDVI changes and their relationships with climatic parameters in Northeast China," *Int. J. Appl. Earth Observ. Geoinf.*, vol. 18, pp. 528–536, Aug. 2012, doi: [10.1016/j.jag.2011.10.007](https://doi.org/10.1016/j.jag.2011.10.007).
- [59] Y. Wei, M. Yu, J. Wei, and B. Zhou, "Impacts of extreme climates on vegetation at middle-to-high latitudes in Asia," *Remote Sens.*, vol. 15, no. 5, p. 1251, Feb. 2021.
- [60] C. E. Bitá and T. Gerats, "Plant tolerance to high temperature in a changing environment: Scientific fundamentals and production of heat stress-tolerant crops," *Frontiers Plant Sci.*, vol. 4, p. 273, Jul. 2013.
- [61] K. Y. Crous, "Plant responses to climate warming: Physiological adjustments and implications for plant functioning in a future, warmer world," *Amer. J. Botany*, vol. 106, no. 8, pp. 1049–1051, Aug. 2019, doi: [10.1002/ajb2.1329](https://doi.org/10.1002/ajb2.1329).
- [62] D. B. Kell, "Breeding crop plants with deep roots: Their role in sustainable carbon, nutrient and water sequestration," *Ann. Botany*, vol. 108, no. 3, pp. 407–418, Sep. 2011, doi: [10.1093/aob/mcr175](https://doi.org/10.1093/aob/mcr175).
- [63] D. Liu, C. Zhang, R. Ogaya, M. Fernández-Martínez, T. A. M. Pugh, and J. Peñuelas, "Increasing climatic sensitivity of global grassland vegetation biomass and species diversity correlates with water availability," *New Phytologist*, vol. 230, no. 5, pp. 1761–1771, Jun. 2021, doi: [10.1111/nph.17269](https://doi.org/10.1111/nph.17269).
- [64] W. Guo, H. Liu, and X. Wu, "Vegetation greening despite weakening coupling between vegetation growth and temperature over the boreal region," *J. Geophys. Res., Biogeosci.*, vol. 123, no. 8, pp. 2376–2387, Aug. 2018, doi: [10.1029/2018JG004486](https://doi.org/10.1029/2018JG004486).
- [65] S. Piao et al., "Evidence for a weakening relationship between interannual temperature variability and northern vegetation activity," *Nature Commun.*, vol. 5, no. 1, p. 5018, Oct. 2014, doi: [10.1038/ncomms6018](https://doi.org/10.1038/ncomms6018).
- [66] R. A. Pielke Sr., R. Avissar, M. Raupach, A. J. Dolman, X. Zeng, and A. S. Denning, "Interactions between the atmosphere and terrestrial ecosystems: Influence on weather and climate," *Global Change Biol.*, vol. 4, no. 5, pp. 461–475, Jun. 1998, doi: [10.1046/j.1365-2486.1998.t01-1-00176.x](https://doi.org/10.1046/j.1365-2486.1998.t01-1-00176.x).

- [67] L. Yu, Y. Xue, and I. Diallo, "Vegetation greening in China and its effect on summer regional climate," *Sci. Bull.*, vol. 66, no. 1, pp. 13–17, Jan. 2021, doi: [10.1016/j.scib.2020.09.003](https://doi.org/10.1016/j.scib.2020.09.003).



JIAPEI WU was born in Bijie, Guizhou, China, in 2000. He received the bachelor's degree from the School of Geographic Science and Planning, Sun Yat-sen University, in 2022. He is currently pursuing the master's degree in cartography and geographic information systems with the Institute of Geographic Sciences and Natural Resources Research, Chinese Academy of Sciences.

His research interests include remote sensing of ecological environment and causal inference.



YUKE ZHOU was born in Jining, Shandong, China, in 1984. He received the Ph.D. degree in cartography and geographic information systems from the Institute of Geographical Sciences and Natural Resources Research, Chinese Academy of Sciences, Beijing, China, in 2013.

He is currently an Associate Researcher with the Institute of Geographical Sciences and Natural Resources Research, CAS. His research interests include high performance geo-computing and development and remote sensing of ecosystem environment.



HAN WANG was born in Nanchong, Sichuan, in 2000. She received the bachelor's degree in geographic information science from the School of Geosciences, Chengdu University of Technology, in 2021. She is currently pursuing the master's degree in cartography and geographic information systems with the Institute of Geographic Sciences and Natural Resources Research, Chinese Academy of Sciences.

Her research interests include ecological environment remote sensing and trend analysis.



XIAOYING WANG was born in Shenyang, Liaoning, China, in 1974. She received the Ph.D. degree in ecology from the Institute of Applied Ecology, Chinese Academy of Sciences, Shenyang, China, in 2003.

She is currently an Associate Researcher with the Institute of Atmospheric Environment, CMA. Her research interests include the impact and adaptation of climate change on natural ecosystems and land-atmosphere interaction.



JIAOJIAO WANG was born in Xiamen, Fujian, China, in 1981. She received the Ph.D. degree in photogrammetry and remote sensing from the College of Geoscience and Surveying Engineering, China University of Mining & Technology-Beijing, China, in 2013. She is currently an Associate Professor with the Institute of Automation, Chinese Academy of Sciences. Her research interests include social computing, infectious diseases informatics, public health management, and artificial intelligence technology empowerment.

• • •